Monthly Notices
of the
ROYAL ASTRONOMICAL SOCIETY

Mon. Not. R. Astron. Soc. **404,** 305–317 (2010) doi:10.1111/j.1365-2966.2010.16280.x

SN 2008iy: an unusual Type IIn Supernova with an enduring 400-d rise time

A. A. Miller,[1⋆] J. M. Silverman,[1] N. R. Butler,[1] J. S. Bloom,[1]† R. Chornock,[1,2] A. V. Filippenko,[1] M. Ganeshalingam,[1] C. R. Klein,[1] W. Li,[1] P. E. Nugent,[3] N. Smith[1] and T. N. Steele[1]

[1]*Department of Astronomy, University of California, Berkeley, CA 94720-3411, USA*
[2]*Harvard–Smithsonian Center for Astrophysics, 60 Garden Street, Cambridge, MA 02138, USA*
[3]*Lawrence Berkeley National Laboratory, 1 Cyclotron Road, Berkeley, CA 94720, USA*

Accepted 2009 December 30. Received 2009 December 27; in original form 2009 November 25

ABSTRACT

We present spectroscopic and photometric observations of the Type IIn supernova (SN) 2008iy. SN 2008iy showed an unprecedentedly long rise time of ∼400 d, making it the first known SN to take significantly longer than 100 d to reach peak optical luminosity. The peak absolute magnitude of SN 2008iy was $M_r \approx -19.1$ mag, and the total radiated energy over the first ∼700 d was $\sim 2 \times 10^{50}$ erg. Spectroscopically, SN 2008iy is very similar to the Type IIn SN 1988Z at late times and, like SN 1988Z, it is a luminous X-ray source (both SNe had an X-ray luminosity $L_X > 10^{41}$ erg s^{-1}). SN 2008iy has a growing near-infrared excess at late times similar to several other SNe IIn. The Hα emission-line profile of SN 2008iy shows a narrow P Cygni absorption component, implying a pre-SN wind speed of ∼100 km s^{-1}. We argue that the luminosity of SN 2008iy is powered via the interaction of the SN ejecta with a dense, clumpy circumstellar medium. The ∼400-d rise time can be understood if the number density of clumps increases with distance over a radius $\sim 1.7 \times 10^{16}$ cm from the progenitor. This scenario is possible if the progenitor experienced an episodic phase of enhanced mass loss <1 century prior to explosion or if the progenitor wind speed increased during the decades before core collapse. We favour the former scenario, which is reminiscent of the eruptive mass-loss episodes observed for luminous blue variable (LBV) stars. The progenitor wind speed and increased mass-loss rates serve as further evidence that at least some, and perhaps all, Type IIn SNe experience LBV-like eruptions shortly before core collapse. We also discuss the host galaxy of SN 2008iy, a subluminous dwarf galaxy, and offer a few reasons why the recent suggestion that unusual, luminous SNe preferentially occur in dwarf galaxies may be the result of observational biases.

Key words: circumstellar matter – stars: mass-loss – supernovae: general – supernovae: individual: SN 2008iy – supernovae: individual: SN 1988Z.

1 INTRODUCTION

The recent development of synoptic, wide-field imaging has revealed an unexpected diversity of transient phenomena. One such example is the discovery of a new subclass of very luminous supernovae (VLSNe; e.g. Ofek et al. 2007; Quimby et al. 2007b; Smith et al. 2007). While events of this nature are rare (Miller et al. 2009; Quimby et al. 2009), each new discovery serves to bracket our understanding of the physical origin of well-established classes of supernovae (SNe) and does, in principle, demand an increased clarity in our understanding of the post-main-sequence evolution of massive stars.

Yet another unusual transient was discovered by the Catalina Real-Time Transient Survey (CRTS; Drake et al. 2009a), which they announced via an ATel as CSS080928:160837+041626 on 2008 October 07 UT[1] (Drake et al. 2008). The transient was classified as a Type IIn SN with a spectrum taken on 2009 March 27 (Mahabal et al.

⋆E-mail: amiller@astro.berkeley.edu
†Sloan Research Fellow.

[1]UT dates are used throughout this paper unless otherwise noted.

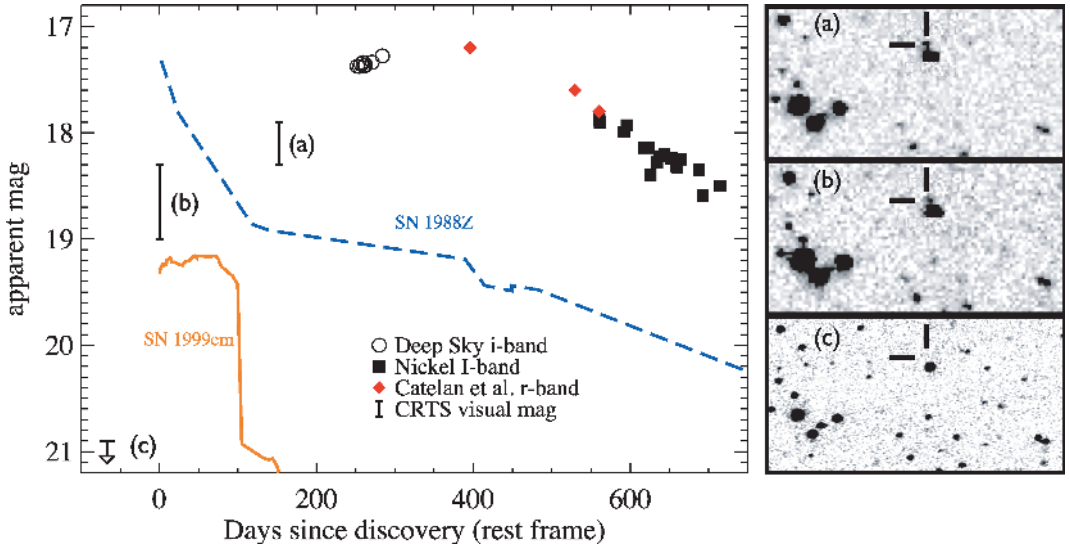

Figure 1. Left: apparent optical light curve of SN 2008iy showing the long rise time of the SN, including data from DS (this work), the Nickel telescope (this work), Catelan et al. (2009) and the CRTS web site. Note, conservatively, we take the start time of the SN ($t = 0$) to coincide with the first epoch where CRTS detects the source; however, the true explosion date is likely prior to 2007 September 13, between the last DS non-detection and the first CRTS detection. Note that the light curve is very broad, and almost symmetric about the peak. For comparison, we show the light curve of the standard Type II-P SN 1999em (data from Leonard et al. 2002) and the Type IIn SN 1988Z, which shows many similarities to SN 2008iy at late times (see Section 3.2; SN 1988Z data from Turatto et al. 1993), as they would have appeared at the redshift of SN 2008iy. Right: three panels with images of the field of SN 2008iy. Each image is $\sim$2.5 $\times$ 4 arcmin^2, with north up and east to the left. Black cross-hairs mark the location of the SN. The bottom image, marked (c), shows the last non-detection from the DS data. The middle (b) and top (a) images show the CRTS detections on days 0 and 153, respectively; SN 2008iy can clearly be seen in each of them. The SN was not flagged as a transient in either the middle or top image by the CRTS software.

2009; see Schlegel 1996 for a definition of the SN IIn subclass, and Filippenko 1997 for a review of the spectral properties of SNe). The SN was later given the IAU designation SN 2008iy (Catelan et al. 2009). Mahabal et al. (2009) noted that the transient was present on CRTS images dating back to 2007 September 13; however, it went undetected by the CRTS automated transient detection software until 2008 because it was blended with a non-saturated, nearby ($\sim$11-arcsec separation) star.

Here, we present our observations and analysis of SN 2008iy, which peaked around 2008 October 29 (Catelan et al. 2009) and had a rise time of $\sim$400 d. This implies that SN 2008iy took longer to reach peak optical brightness than any other known SN. Type II SN rise times are typically $\lesssim$1 week [e.g. SNe 2004et and 2006bp; Li et al. 2005; Quimby et al. 2007a; see also Patat et al. 1993; Li et al., in preparation(a)], and have never previously been observed to rise $\gtrsim$100 d, let alone 400, making SN 2008iy another rare example of the possible outcomes for the end of the stellar life cycle. In addition to an extreme rise time, SN 2008iy is of great interest because the unique circumstellar medium (CSM) in which it exploded may provide a link to very long-lived SNe, such as SN 1988Z, and thus provide clues into the nature of their progenitors.

This paper is organized as follows. Section 2 presents the observations. The data are analysed in Section 3, and the results are discussed in Section 4. We give our conclusions, as well as predictions for the future behaviour of SN 2008iy, in Section 5.

2 OBSERVATIONS

2.1 Photometry

The field of SN 2008iy, which is located at $\alpha = 16^{\rm h}08^{\rm m}37\overset{\rm s}{.}27$, $\delta = +04^\circ16'26\overset{''}{.}5$ (J2000), was imaged multiple times by the Palomar Quest survey, and those data have been reprocessed as part of the Deep Sky (DS) project[2] (Nugent 2009). The best constraints on the explosion date come from DS imaging: in a co-add of two images from 2007 July 05, we do not detect the SN down to a 3σ limit of $i > 20.9$ mag. DS images are best approximated by the Sloan Digital Sky Survey (SDSS; Adelman-McCarthy et al. 2008) i-band filter. The field of SN 2008iy has well-calibrated SDSS photometry which we use to calibrate the DS images. The observed DS magnitudes are shown in Fig. 1 and summarized in Table 1.

Table 1. DS Observations of SN 2008iy.

Date (MJD)	Mag [a]	$\sigma_{\rm mag}$ [b]
54618.35	17.37	0.12
54621.35	17.38	0.12
54623.33	17.35	0.12
54626.32	17.34	0.12
54627.36	17.37	0.12
54628.29	17.37	0.12
54629.30	17.36	0.12
54638.21	17.34	0.12
54651.20	17.28	0.12

[a]Observed value; not corrected for Galactic extinction.
[b]The calibration uncertainty dominates over the statistical uncertainty with values of $\sim$0.12 and $\sim$0.01 mag, respectively.

To constrain the rise time of SN 2008iy, we visually estimate the possible range of magnitudes for the SN from images on the CRTS

[2]http://supernova.lbl.gov/~nugent/deepsky.html

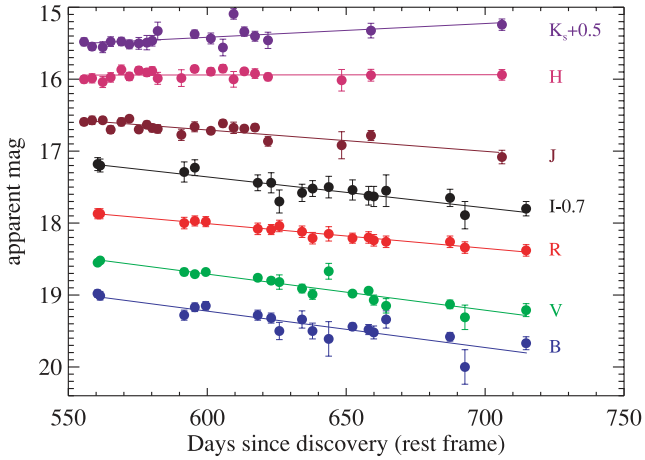

Figure 2. Filtered photometry including *BVRI* from the Nickel telescope and J, H and K_s from PAIRITEL, showing the decline rate of SN 2008iy between days ∼560 and 715. To help guide the eye, we illustrate the linear fit to each band used to determine the photometric decline rates (see the text). Note that the single epoch of UVOT B- and V-band observations we measured, which agree to $<1\sigma$ with Nickel data taken <2 d later, is not shown in this figure.

website[3] based on a comparison to SDSS images. As previously mentioned, SN 2008iy is blended with a nearby star and so the automated photometry produced by the CRTS does not detect the SN on these epochs. On 2007 September 13, the SN was between 18.3 and 19.0 mag, while on 2008 February 19 the SN was observed between 17.9 and 18.3 mag.

Near-infrared (NIR) observations of SN 2008iy were conducted with the 1.3-m Peters Automated Infrared Imaging Telescope (PAIRITEL; Bloom et al. 2006) starting on 2009 April 13. PAIRITEL observes simultaneously in the J, H and K_s bands. Observations were scheduled and executed via a robotic system, and the data were reduced by an automated pipeline (Bloom et al. 2006). The SN flux was measured via aperture photometry using SExtractor (Bertin & Arnouts 1996), calibrated against the Two-Micron All-Sky Survey (2MASS; Skrutskie et al. 2006). Filtered photometry of SN 2008iy is shown in Fig. 2 and summarized in Table 2.

Ground-based optical observations of SN 2008iy were obtained using the 1.0-m Nickel telescope located at Lick Observatory (Mt. Hamilton, CA, USA) starting on 2009 April 18. *BVRI* photometry from the Nickel was measured using the daophot package (Stetson 1987) in iraf,[4] and transformed into the Johnson–Cousins system. Calibrations for the field were obtained on 10 photometric nights with the Nickel telescope. The Nickel photometry is shown in Fig. 2 and summarized in Table 3.

SN 2008iy was observed by the space-based *Swift* observatory on 2009 April 15 and 16. *Swift* observed the SN simultaneously with both the X-ray Telescope (XRT; Burrows et al. 2005) and the Ultraviolet/Optical Telescope (UVOT; Roming et al. 2005). We downloaded the Level-2 UVOT images, and measured the U, B and V photometry using the recipe of Li et al. (2006). The UV filters (*UVM*1, *UVW*1 and *UVW*2) were calibrated using the method of Poole et al. (2008). Our final UVOT photometry is summarized in Table 4. The XRT observed the field for a total of 10.71 ks. We extract the 0.3–10.0 keV counts from an extraction region of 64 pixels (∼2.5 arcmin), where we fit the point-spread function model (see Butler & Kocevski 2007) at the centroid of the X-ray emission. From the native XRT astrometry, the centroid of the X-ray emission, located at $\alpha = 16^{\rm h}08^{\rm m}37\overset{\rm s}{.}23$, $\delta = +04^\circ16'26\overset{''}{.}7$ (J2000), with a radial uncertainty of 5 arcsec (90 per cent confidence interval), coincides with the optical position of SN 2008iy, suggesting that the X-rays are from the SN. In an astrometric fit relative to 2MASS, we measure the position of the star ∼11 arcsec from the SN to be $\alpha = 16^{\rm h}08^{\rm m}36\overset{\rm s}{.}98$, $\delta = +04^\circ16'16\overset{''}{.}4$ (J2000), with an rms scatter of 0.19 arcsec in α and 0.18 arcsec in δ for our astrometric

[3]http://crts.caltech.edu/

[4]iraf is distributed by the National Optical Astronomy Observatory, which is operated by the Association of Universities for Research in Astronomy under cooperative agreement with the National Science Foundation (NSF).

Table 2. PAIRITEL observations of SN 2008iy.

$t_{\rm mid}$[a] (MJD)	J mag[b] (Vega)	H mag[b] (Vega)	K_s mag[b] (Vega)
54934.42	16.59 ± 0.05	16.00 ± 0.05	14.98 ± 0.05
54937.43	16.57 ± 0.06	15.99 ± 0.06	15.05 ± 0.05
54941.43	16.57 ± 0.05	16.04 ± 0.08	15.06 ± 0.08
54944.40	16.70 ± 0.05	15.98 ± 0.07	14.98 ± 0.07
54948.40	16.59 ± 0.05	15.87 ± 0.06	14.98 ± 0.06
54951.39	16.55 ± 0.04	15.96 ± 0.06	15.02 ± 0.06
54954.35	16.70 ± 0.04	15.88 ± 0.05	15.00 ± 0.08
54957.37	16.63 ± 0.05	15.91 ± 0.05	14.99 ± 0.10
54959.37	16.68 ± 0.05	15.89 ± 0.06	14.97 ± 0.07
54961.44	16.69 ± 0.06	15.99 ± 0.08	14.83 ± 0.12
54970.30	16.77 ± 0.08	15.98 ± 0.12	...
54975.28	16.66 ± 0.07	15.86 ± 0.05	14.87 ± 0.06
54981.35	16.72 ± 0.04	15.90 ± 0.05	14.93 ± 0.08
54986.29	16.61 ± 0.05	15.85 ± 0.06	15.06 ± 0.12
54990.30	16.68 ± 0.08	16.00 ± 0.11	14.59 ± 0.07
54994.30	16.69 ± 0.05	15.89 ± 0.04	14.84 ± 0.06
54998.31	16.67 ± 0.05	15.92 ± 0.07	14.90 ± 0.07
55003.18	16.86 ± 0.07	15.97 ± 0.05	14.96 ± 0.11
55030.20	16.92 ± 0.19	16.01 ± 0.15	...
55041.18	16.78 ± 0.07	15.94 ± 0.08	14.82 ± 0.10
55091.10	17.08 ± 0.09	15.94 ± 0.07	14.74 ± 0.08

[a]Midpoint between the first and last exposures in a single stacked image.
[b]Observed value; not corrected for Galactic extinction.

Table 3. Nickel Observations of SN 2008iy.

Date (MJD)	B mag[a] (Vega)	V mag[a] (Vega)	R mag[a] (Vega)	I mag[a] (Vega)
54939.52	19.06 ± 0.01	18.59 ± 0.03	17.86 ± 0.01	17.87 ± 0.03
54940.46	19.09 ± 0.03	18.56 ± 0.02	17.86 ± 0.02	17.89 ± 0.03
54971.37	19.35 ± 0.06	18.71 ± 0.04	17.99 ± 0.04	17.98 ± 0.11
54975.36	19.25 ± 0.03	18.75 ± 0.02	17.96 ± 0.02	17.92 ± 0.07
54979.46	19.23 ± 0.03	18.71 ± 0.02	17.97 ± 0.02	–
54999.35	19.36 ± 0.05	18.79 ± 0.03	18.07 ± 0.03	18.12 ± 0.08
55004.37	19.40 ± 0.05	18.84 ± 0.03	18.07 ± 0.02	18.13 ± 0.11
55007.43	19.56 ± 0.11	18.84 ± 0.10	18.02 ± 0.04	18.37 ± 0.13
55015.36	19.43 ± 0.11	18.95 ± 0.06	18.10 ± 0.04	18.26 ± 0.08
55019.30	19.58 ± 0.09	19.02 ± 0.06	18.19 ± 0.03	18.21 ± 0.07
55025.36	19.66 ± 0.24	18.66 ± 0.10	18.16 ± 0.08	18.18 ± 0.12
55034.26	19.52 ± 0.02	19.02 ± 0.03	18.19 ± 0.02	18.23 ± 0.11
55040.30	19.56 ± 0.05	18.97 ± 0.03	18.18 ± 0.03	18.30 ± 0.09
55042.24	19.60 ± 0.07	19.11 ± 0.06	18.21 ± 0.03	18.31 ± 0.11
55047.27	19.43 ± 0.11	19.21 ± 0.10	18.22 ± 0.04	18.24 ± 0.20
55071.22	19.66 ± 0.04	19.17 ± 0.05	18.23 ± 0.03	18.34 ± 0.09
55077.23	20.07 ± 0.24	19.33 ± 0.17	18.29 ± 0.03	18.58 ± 0.17
55100.15	19.75 ± 0.07	19.25 ± 0.08	18.35 ± 0.03	18.49 ± 0.06

[a]Observed value; not corrected for Galactic extinction.

Table 4. UVOT observations of SN 2008iy.

$t_{\rm mid}$ [a] (MJD)	Filter	Mag [b] (Vega)	$\sigma_{\rm mag}$
54936.31	*UVW2*	19.14	0.06
54936.32	*UVM2*	18.95	0.08
54936.32	*UVW1*	18.53	0.07
54936.31	*U*	18.60	0.06
54937.49	*UVW2*	19.12	0.04
54937.85	*B*	19.04	0.06
54937.85	*V*	18.65	0.08

[a]Midpoint between the first and last exposures in a single stacked image.
[b]Observed value; not corrected for Galactic extinction.

solution. This star is therefore well outside the 90 per cent confidence interval for the location of the X-ray emission. Furthermore, there is no catalogued X-ray source at the position of the SN in the *ROSAT* catalogue (Voges et al. 1999), also suggesting that the star located ∼11 arcsec from the SN is not the source of X-ray emission. We measure a background-subtracted 0.3–10.0 keV count rate of $(19 \pm 6) \times 10^{-4}$ counts s^{-1}.

2.2 Spectroscopy

Spectra of SN 2008iy were obtained on 2009 April 18, 25 and 2009 July 23 with the Kast spectrograph on the Lick 3-m Shane telescope (Miller & Stone 1993). An additional spectrum was obtained on 2009 September 22 with the Low-Resolution Imaging Spectrometer (LRIS; Oke et al. 1995) on the 10-m Keck I telescope. To improve the spectral resolution at the location of the Hα emission feature from SN 2008iy, we used the 1200 lines mm^{-1} grating on the red side of the double-arm (blue+red) LRIS system. The spectra were reduced and calibrated using standard procedures (e.g. Matheson et al. 2000). Clouds were present on the night of 2009 April 25, and the observing setup from that night did not include any wavelength overlap between the red and blue arms of the Kast spectrograph; thus, the absolute flux calibration on this night is less certain than on the other nights. For the Kast spectra, we observed the SN with the slit placed at the parallactic angle, so the relative spectral shapes should be accurate (Filippenko 1982). LRIS is equipped with an atmospheric dispersion corrector; nevertheless, we observed the SN at the parallactic angle on this night as well. In Fig. 3, we show the spectral sequence of SN 2008iy, and a summary of our observations is given in Table 5.

Table 5. Log of spectroscopic observations.

Epoch [a]	UT Date	Telescope/ instrument	Exposure (s)
560	2009-04-18.458	Shane 3-m/Kast	1500
567	2009-04-25.479	Shane 3-m/Kast	1500
652	2009-07-23.274	Shane 3-m/Kast	1800
711	2009-09-22.236	Keck I 10-m/LRIS	600

[a]Defined as rest-frame days relative to day 0, 2007 September 13.

2.3 Host galaxy

There is no catalogued redshift for the host galaxy of SN 2008iy. To determine the redshift of the SN, we examined the LRIS spectrum for the presence of narrow emission lines. Based on a fit to the [O III] λλ4959, 5007 doublet, we adopt a heliocentric redshift of $z = 0.0411$ for SN 2008iy (not corrected for peculiar motions or Virgo infall). This corresponds to a luminosity distance of $d_{\rm L} = 179$ Mpc ($H_0 = 71$ km s^{-1} Mpc^{-1}, $\Omega_{\rm M} = 0.27$, $\Omega_\Lambda = 0.73$), which we adopt throughout the remainder of this paper.

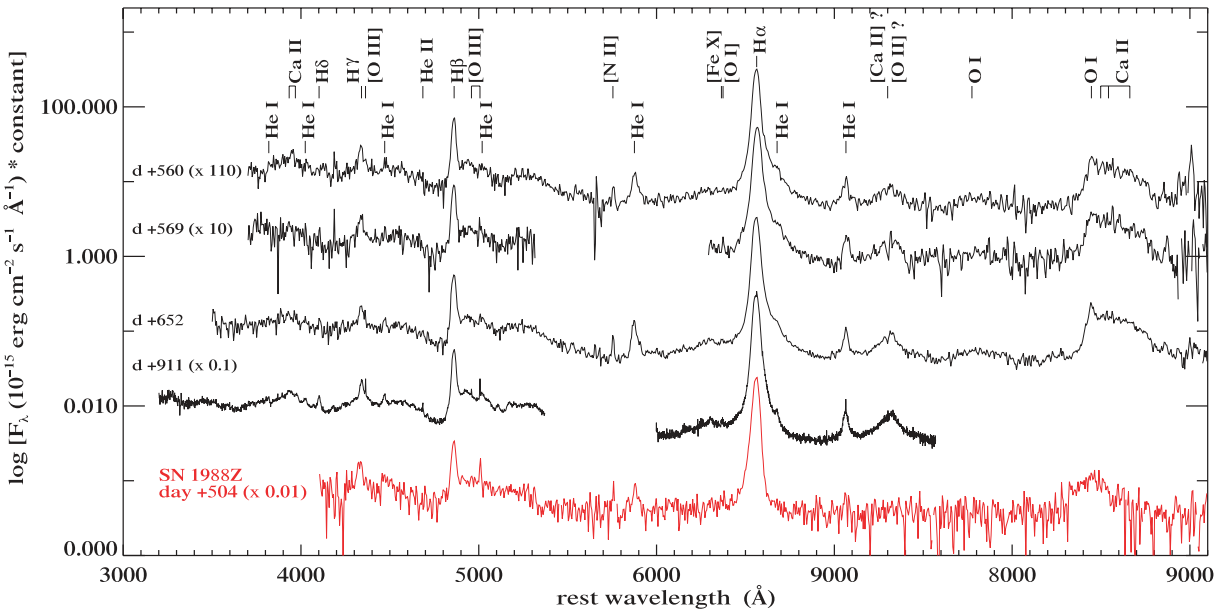

Figure 3. Spectral sequence of SN 2008iy (shown in black) and a single, late-time spectrum of SN 1988Z from our spectral data base (shown in red), which was observed 504 d after discovery. To the left of the spectra, we give the time since discovery, in rest-frame days, at which each spectrum was taken. Prominent spectral features of SN 2008iy are labelled at the top of the figure. The spectra show little evolution between days 560 and 711. Fe II multiplets 42, 48 and 49 can also be seen, though we have not labelled those lines. The spectra have been corrected for Galactic reddening [$E(B - V) = 0.065$ mag; Schlegel, Finkbeiner & Davis 1998]. We have assumed no reddening in the SN host galaxy (see Section 2.3).

The reddening of SN 2008iy by the host galaxy is uncertain. In our Kast spectra, we do not detect any absorption from Na I D, and therefore we adopt $A_{\lambda,\rm host} = 0$ mag.

We confirm the possible detection of the host galaxy by Catelan et al. (2009) in a stack of SDSS *g*-, *r*- and *i*-band images of the field. When the $g + r + i$ stack is calibrated to the SDSS *r*-band, we find that the host has $r = 22.75 \pm 0.15 \pm 0.08$ mag in a 2.2 arcsec diameter aperture, where the two errors represent the statistical and calibration uncertainties, respectively.

As first noted by Catelan et al. (2009), the field of SN 2008iy was observed by the Galaxy Evolution Explorer (Martin et al. 2005). On 2004 May 17, the field was imaged as part of the all-sky imaging survey; the host was not detected to a 5σ limiting magnitude of far-ultraviolet (FUV) $\gtrsim 20.2$ and near-ultraviolet (NUV) $\gtrsim 20.5$ mag. The field was re-imaged as part of the medium imaging survey on 2008 June 05/06, and SN 2008iy was detected at FUV $= 21.175 \pm 0.094$ mag and NUV $= 19.929 \pm 0.036$ mag.

3 RESULTS

3.1 Photometric analysis

At $z = 0.0411$, the absolute peak magnitude of SN 2008iy was a relatively modest $M_r \approx -19.1$ mag. This places SN 2008iy well below the most luminous SNe IIn, such as SN 2006gy ($M_R = -21.7$ mag; Ofek et al. 2007; Smith et al. 2007) and SN 2008fz ($M_V = -22.3$ mag; Drake et al. 2009b), and more in the range of the well-studied SN IIn 1988Z ($M_R \lesssim -18.9$ mag; Turatto et al. 1993; Stathakis & Sadler 1991). Assuming no bolometric correction, the total integrated optical output from SN 2008iy during the first $\sim$700 d after discovery is $\sim 2 \times 10^{50}$ erg. Between day 550 and 720, the SN declines in the optical and the *J* band, while it actually gets brighter in the *H* and K_s bands. During this time, the linear decay rates are as follows: $\beta_B = 0.51$ mag $(100\ {\rm d})^{-1}$, $\beta_V = 0.50$ mag $(100\ {\rm d})^{-1}$, $\beta_R = 0.34$ mag $(100\ {\rm d})^{-1}$, $\beta_I = 0.43$ mag $(100\ {\rm d})^{-1}$, $\beta_J = 0.30$ mag $(100\ {\rm d})^{-1}$, $\beta_H = -0.03$ mag $(100\ {\rm d})^{-1}$ and $\beta_{K_s} = -0.19$ mag $(100\ {\rm d})^{-1}$. These decline rates, all slower than the expected rate of decline for radioactive ^{56}Co, 0.98 mag $(100\ {\rm day})^{-1}$, strongly suggest that the SN is still being powered by CSM interaction $\sim$700 d after explosion.

For comparison purposes, in addition to the light curve of SN 2008iy, Fig. 1 shows the light curve of the standard Type II-P SN 1999em (Leonard et al. 2002) as it would have appeared at the redshift of SN 2008iy. As well as illustrating the very long rise time of SN 2008iy, this comparison shows that SN 2008iy was fairly luminous at the time of discovery. Thus, despite the sparse sampling over the first $\sim$200 d, this large luminosity suggests that the early detections are not related to a pre-SN outburst, as was observed for SN 2006jc (Foley et al. 2007; Pastorello et al. 2007). CRTS images indicate that the SN was rising over the first $\sim$400 d (Mahabal et al. 2009), which provides further evidence against a pre-SN outburst. Fig. 1 also shows the light curve of the long-lived, interacting, Type IIn SN 1988Z (Turatto et al. 1993). The explosion date of SN 1988Z is not well constrained (see Section 4.3), so we shift the first epoch of detection to day 0. Note the similarity of the decline rate of SN 2008iy and SN 1988Z around day $\sim$600; these SNe also have very similar late-time spectra (see Section 4.2).

We were unable to fit the UV through NIR spectral energy distribution (SED) of SN 2008iy to a single-temperature blackbody model. This is not surprising, as SNe II are dominated by emission lines at late times, and single-temperature blackbody models typically apply only to young SNe II (see e.g. Filippenko 1997). Direct integration of the UV–NIR SED shows that the bolometric correction, relative to the *I* band, is a factor of $\sim$3 in luminosity, corresponding to $\sim$1.2 mag, on day $\sim$560. Some features stand out from the SED: there is a strong *R*-band excess relative to the other optical bands, with $V - R = 0.8$ mag and $R - I = -0.2$ mag on day 715. The red $V - R$ colour relative to a blue $R - I$ colour can be attributed to the Hα emission with large equivalent width. This emission also accounts for the relatively slow decay rate in the *R* band, as compared to the other optical bands. There is also an NIR excess relative to the *I*-band flux. In fact, this excess increases with time, $I - K_s \approx 2.8$ mag on day $\sim$560 and $I - K_s \approx 3.7$ mag on day $\sim$710, which is indicative of the growing importance of dust in the emission from SN 2008iy.

An NIR excess at late times has been observed in many SNe IIn (e.g. Gerardy et al. 2002), and it is the result of either new dust formation (e.g. SN 2005ip; Smith et al. 2009; Fox et al. 2009) or the presence of an NIR light echo from pre-existing dust (Dwek 1983), or both. To distinguish between these two possibilities, which are virtually identical from photometry alone, requires well-sampled optical spectra (see Section 3.2.2) since line profiles are expected to change with time if new dust is being formed. On day 706, corresponding to our last PAIRITEL observation, the $H - K_s$ colour of SN 2008iy was $\sim$1.2 mag. Assuming that the dust radiates as a perfect blackbody, this colour corresponds to a dust temperature of $T_{\rm dust} \approx 1320$ K, while the K_s-band measurement corresponds to a dust luminosity $L_{\rm NIR} \approx 4.8 \times 10^{42}$ erg s^{-1}, assuming no bolometric correction as we cannot constrain the emission in the mid-IR. This luminosity is very large, though upon making similar assumptions Gerardy et al. (2002) found NIR luminosities $> 10^{42}$ erg s^{-1} for SNe 1995N and 1997ab at late times. Gerardy et al. also found that the NIR luminosity was roughly an order of magnitude greater than the X-ray emission from SN 1995N, which is also the case for SN 2008iy (see Section 3.3). The $H - K_s$ colour of SN 2008iy is bluer than those of the Gerardy et al. sample at a similar epoch, which may be a result of the long rise of SN 2008iy or a contribution to the NIR emission from the SN in addition to the dust. Future NIR observations, as the underlying SN light continues to fade, will place more stringent constraints on the dust near SN 2008iy.

3.2 Spectroscopic analysis

Our spectra of SN 2008iy at ages >560 d are very similar to those of an unpublished spectrum, from our spectral data base, of the Type IIn SN 1988Z taken at a comparable epoch, as shown in Fig. 3. The general features resemble those of several other SNe IIn (Filippenko 1997): there are prominent Balmer and He I emission lines, most notably the dominant Hα emission, which primarily feature intermediate-width emission components with full width at half-maximum intensity (FWHM) $\sim$1650 km s^{-1} in the case of SN 2008iy. The higher resolution Keck spectrum reveals a number of narrow, marginally resolved (FWHM $\lesssim 170$ km s^{-1}) emission lines, including Hα, Hβ, [O III] $\lambda\lambda$4363, 4959, 5007 and He I λ7065. The only high-ionization line we detect is [Fe X] λ6375. The relative lack of narrow forbidden lines and the low intensity ratio of [O III] $\lambda\lambda$4959, 5007 to [O III] λ4363 suggest a large electron density for the ejecta (Filippenko & Halpern 1984; Filippenko 1989; Stathakis & Sadler 1991). The relative spectral features do not show strong evolution between days 560 and 711.

We can estimate the density of the unshocked emitting material based on the relative intensities of the three [O III] lines mentioned above. Note that [O III] λ4363 is only resolved in our day 711 Keck spectrum, so the following estimate of the density is at that epoch

only. Following a removal of the underlying continuum, we fit three Gaussian profiles to [O III] λ4363 and [O III] λλ4959, 5007, and find that $\mathcal{R} = I[\lambda4959+\lambda5007]/I[\lambda4363] \approx 1.7$. As mentioned above, the strong presence of [O III] λ4363 indicates a high density for the emitting material. In fact, with $\mathcal{R} \approx 1.7$, the electron density, n_e, must be $>10^6$ cm^{-3} regardless of the temperature of the emitting gas. Typically, [O III] emission comes from photoionized regions with $T = 16\,000$–$20\,000$, in which case $n_e \approx 10^7$ cm^{-3} (see fig. 11 in Filippenko & Halpern 1984). Note that this high-density material is likely only present within clumps in the CSM (see Section 4.2), and that interclump portions of the CSM have a lower density.

3.2.1 *The Hα profile*

As seen in Fig. 3, the Hα emission feature dominates over all the other lines. In the high-resolution Keck spectrum, we see evidence for three distinct emission features: a broad component (FWHM ≈ 4500 km s^{-1}), an intermediate component (FWHM ≈ 1650 km s^{-1}) and a marginally resolved, narrow P Cygni feature (FWHM ≈ 75 km s^{-1}), as shown in Fig. 4. The main panel of Fig. 4 shows a fit to the Hα profile (red line) which includes a broad (FWHM ≈ 4500 km s^{-1}) and an intermediate (FWHM ≈ 1650 km s^{-1}) component. Panel (a) in Fig. 4 shows a close-up view of the narrow emission after the broad and intermediate components have been removed using a spline fit. We fit the spline to the observed Hα profile from -1000 to 1000 km s^{-1} after masking the region between -200 and 200 km s^{-1}. A narrow absorption minimum such as this, located at ~ -100 km s^{-1}, has been seen in a number of typical SNe IIn (e.g. SNe 1997ab, 1997eg and 1998S; Salamanca 2000; Fassia et al. 2001; Salamanca, Terlevich & Tenorio-Tagle 2002), and it traces the outflow velocity of the progenitor wind. We note that while the narrow absorption is only marginally resolved a P Cygni profile with characteristic speeds of $\sim$10 km s^{-1}, typical of red supergiants (RSGs), would go completely unresolved in the Keck spectrum. Therefore, this P Cygni profile must be associated with an outflow velocity that is >10 km s^{-1}, which will have important consequences for the progenitor (see Section 4.3).

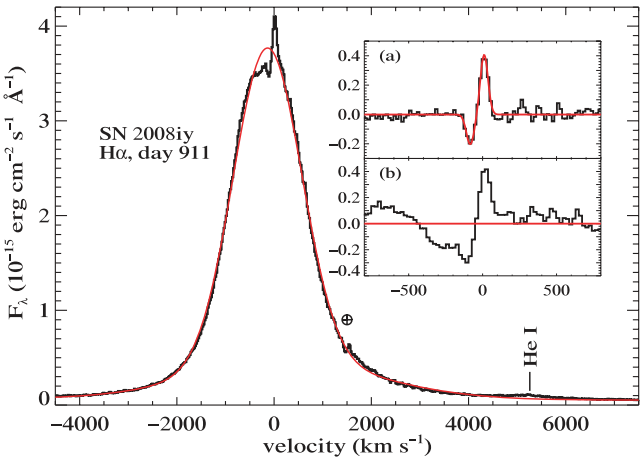

Figure 4. Detailed view of the Hα profile from the Keck spectrum taken on day 711. Main panel: the black line shows the observed Hα profile, while the smooth red line illustrates a two-Gaussian fit (intermediate, FWHM $\approx$ 1650 km s^{-1}; broad, FWHM $\approx$ 4500 km s^{-1}) to the profile. Residual emission and absorption from a narrow component to the profile can easily be seen. The location of He I λ6678 has been marked, and the residuals from an imperfect telluric absorption correction have been marked by the ⊕ symbol. Inset (a): close-up view of the residual, narrow P Cygni component. The smooth red line shows a fit to the feature that includes a Gaussian in emission and a Gaussian in absorption (both Gaussians have FWHM $\approx$ 75 km s^{-1}). The absorption minimum of the narrow absorption is located at -100 km s^{-1}. Note that for this fit we removed the broad plus intermediate components using a spline fit over the region from -1000 to 1000 km s^{-1} (see the text). Inset (b): residuals following the subtraction of the two-Gaussian broad plus intermediate fit from the observed Hα profile. The absorption minimum still occurs at -100 km s^{-1}, but the BVZI extends to ~ -450 km s^{-1}, meaning the progenitor wind speed may be >100 km s^{-1} (see the text).

It is interesting that the broad plus intermediate fit overestimates the Hα flux out to about -450 km s^{-1}. In panel (b) of Fig. 4, we show the residual flux, centred on Hα, following the subtraction of our two-Gaussian fit to the broad plus intermediate emission. The blue velocity at zero intensity (BVZI) extends to roughly -450 km s^{-1}, which means that the true wind speed from the progenitor, as traced by the absorbing gas moving directly along the line of sight towards the SN, may be >100 km s^{-1} and possibly as high as $\sim$450 km s^{-1}. If this feature represents a true lack of emission, it would be evidence for a two-component CSM: one with velocity $v_{w,1} \approx 100$ km s^{-1} and the other with BVZI $\approx v_{w,2} \approx 450$ km s^{-1}. Similar features were seen in SN 1998S (Fassia et al. 2001), which were modelled by Chugai et al. (2002) to be a slow wind accelerated to higher velocities by radiation from the SN photosphere, and in SN 2006gy, which Smith et al. (2010) argued was the result of a CSM shell that had been ejected from the progenitor in a pre-SN eruption. These two scenarios predict different behaviour as the SN evolves.

In the radiatively accelerated scenario, as shown by Chugai et al. (2002) for SN 1998S, the second, faster component to the wind has a negative velocity gradient. Observationally, this effect manifests itself as a BVZI for the second, faster CSM component that decreases with time, as observed in SN 1998S (Fassia et al. 2001). In the shell-ejection scenario, the wind exhibits a positive velocity gradient as the ejected shell is freely expanding, which is thought to be the result of an explosive ($\sim 10^{49}$–10^{50} erg) mass-loss event (see e.g. Chugai et al. 2004). This scenario leads to a BVZI that increases with time, as was observed for SN 2006gy (Smith et al. 2010). With only a single high-resolution spectrum, we are unable to probe the evolution of this feature, but we note that the velocity of a radiatively accelerated CSM is proportional to t^{-2} (Fransson, Lundqvist & Chevalier 1996), so this mechanism is unlikely to be significant at late times (>a few hundred days).

As does the overall continuum, the Hα luminosity declines over the course of our observations. In Table 6, we summarize the observed properties of the Hα profile from our spectra on days 560, 652 and 711. We do not include the spectrum from day 567, as it was taken under cloudy conditions and the overall flux scaling is uncertain, but we do not expect significant spectral evolution between days 560 and 567. The decline in the Hα luminosity is accompanied by a rise in the equivalent width over this same time period. For the narrow emission on day 711, we measure $L(\mathrm{H}\alpha) = (2.8 \pm 0.6) \times 10^{39}$ erg s^{-1}, though we note that this value is likely underestimated because the blue emission wing is probably being partially absorbed. The FWHM of the intermediate component is $\sim$1650 km s^{-1} at all epochs, while the FWHM of the broad component drops from $\sim$5800 km s^{-1} on day 560, to $\sim$5200 km s^{-1} on day 650, to $\sim$4400 km s^{-1} on day 711. We attribute this change in the broad component to rapid evolution of the spectrum redwards of Hα between days 560 and 711, as shown in Fig. 5. The nature of this feature is not currently understood: it could potentially be an absorption feature, or it could be related to a lack of emission from some unidentified species. Similar spectral evolution redwards of Hα has been seen in the interacting SNe 2005gj and 2006gy (Prieto

Table 6. Hα line widths, luminosity, equivalent width and ratio to Hβ.

Epoch [a]	Br. FWHM (km s^{-1})	Int. FWHM (km s^{-1})	Nar. FWHM (km s^{-1})	L(Hα) [b] (erg s^{-1})	EW [c] (Å)	Hα/Hβ
560	5774	1641	–	7.86×10^{41}	2122	9.49
652	5162	1685	–	6.10×10^{41}	2386	12.22
711	4405	1639	78	6.50×10^{41}	2786	12.54

[a]Defined as rest-frame days relative to day 0, 2007 September 13.
[b]Uncertainty $\sim \pm 10$ per cent.
[c]Uncertainty $\sim \pm 10$ per cent.

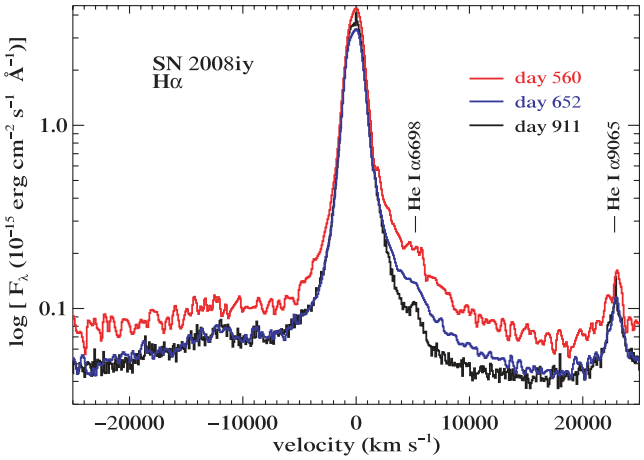

Figure 5. Evolution of the Hα profile of SN 2008iy between days 560 and 711. The profile remains largely unchanged, with the exception of a variable spectral feature between ∼200 and 20 000 km s^{-1}, from day 652 to day 711. Similar spectral features have been observed in other interacting SNe (see the text). Emission lines of He I λ6678 and He I λ7065 are labelled.

et al. 2007; Smith et al. 2010). We do not associate this feature with Hα, as the red velocity at zero intensity corresponds to velocities of $\gtrsim$22 000 km s^{-1}, and there are no other emission lines that show evidence for velocities this large.

3.2.2 He I emission

In addition to the prominent Balmer emission lines, SN 2008iy exhibits several He I lines in emission, including λλ3820, 4026, 4471, 5016, 5875, 6678 and 7065. None of these lines shows evidence for a broad component, and the intermediate component, FWHM ≈ 1100–1400 km s^{-1}, is slightly narrower than that observed for Hα. As previously mentioned, He I λ7065 has a narrow, marginally resolved emission component in addition to the intermediate component.

A systematic, increasing blueshift in the He I profiles has been argued as evidence for dust formation in the cool, dense shell formed in the post-shock gas of the Type IIn SNe 1998S and 2005ip (Pozzo et al. 2004; Smith et al. 2009). Newly formed dust in the post-shock region absorbs light from the receding ejecta, resulting in a suppression of flux from the red side of the emission line. Using He I λ7065, the strongest He line in our spectra, we searched for changes in the red wing of the profile. The Kast spectra from days 560 and 567 are very noisy, but in the higher signal-to-noise ratio spectra from days 652 and 711 we see no evidence for a change in the red wing of the emission profile. This hints that the observed NIR excess (see Section 3.1) is the result of an NIR echo, rather than newly formed dust, though we caution that with only two spectra separated by ∼50 d the lack of change in the He I profile does not constitute definitive evidence for this.

3.3 X-ray analysis

To determine the X-ray luminosity of SN 2008iy, we assume a thermal plasma spectrum with temperature 0.6 keV (see e.g. Immler & Kuntz 2005), which has been absorbed by a Galactic column density of n(H) = 4.8 × 10^{20} cm^{-2} (Kalberla et al. 2005). Using the 0.3–10 keV XRT count rate (see Section 2.1) and PIMMS,[5] we measure the unabsorbed flux, assuming no absorption within the host, to be $(6.1 \pm 1.9) \times 10^{-14}$ erg cm^{-2} s^{-1}. At the adopted distance of SN 2008iy, this corresponds to a luminosity of $L_{\rm X} = (2.4 \pm 0.8) \times 10^{41}$ erg s^{-1}. Note that Fox et al. (2000) fit the late-time (>3 yr) X-ray spectra of SN 1995N with a larger temperature of 9.1 keV, which would correspond to a flux and luminosity of $(9.1 \pm 2.9) \times 10^{-14}$ erg cm^{-2} s^{-1} and $(3.5 \pm 1.1) \times 10^{41}$ erg s^{-1}, respectively, were we to adopt this value for SN 2008iy. Similar luminosities ($L_{\rm X} > 10^{41}$ erg s^{-1}) are observed for other interacting SNe more than 1 yr post explosion (e.g. SNe 1988Z and 1995N; Fox et al. 2000).

4 DISCUSSION

4.1 Mass loss in the SN 2008iy progenitor

We assume that the continuum emission traced by the light curve of SN 2008iy is powered solely by CSM interaction. The half life of ^{56}Ni is $\tau \approx 6.0$ d, much too short to power the >400-d rise of SN 2008iy, while the photometric decay rates are too slow to be powered by ^{56}Co (see Section 3.1), implying that radioactivity contributes minimally to the light curve of SN 2008iy. Furthermore, the SN ejecta will suffer considerable adiabatic losses during the 400-d rise of the light curve, suggesting that interaction is the only viable mechanism for powering SN 2008iy over this entire time.

Following our assumption of interaction-driven luminosity, the expelled gas from the progenitor overtaken by the shock at each epoch can be written as (see Chugai & Danziger 1994)

$$\dot{M} = \frac{2}{\psi} L \frac{v_{\rm w}}{V_{\rm SN}^3}, \quad (1)$$

where $\dot{M}$ is the mass-loss rate of the progenitor, ψ is an efficiency factor describing the conversion of kinetic energy into radiation, L is the luminosity of the SN, $v_{\rm w}$ is the wind speed of the progenitor and $V_{\rm SN}$ is the velocity of the blast wave overrunning the CSM. We adopt $\psi = 0.5$, but this number is likely an overestimate given the optically thin nature of the emission (see Section 4.2). The CSM wind is only probed by our higher resolution spectrum from day 711, so we

[5]http://heasarc.nasa.gov/Tools/w3pimms.html.

adopt $v_w = 100\,\mathrm{km\,s^{-1}}$ based on the narrow P Cygni absorption seen in Hα, though this may not be valid at all times between days 0 and 700 (see below). We adopt $V_{SN} = 5000\,\mathrm{km\,s^{-1}}$ based on the typical widths of the broad Hα emission, which should trace the speed of the blast wave. Unlike our assumption of a constant wind speed, the adoption of a constant-velocity blast wave at all times should at the very least be valid after the peak, at which point the CSM density is decreasing with increasing radius. Hydrodynamic modelling of SNe IIn demonstrates that the blast wave is quickly decelerated to a roughly constant expansion speed as the ejecta sweep up successively more CSM (see e.g. Chugai et al. 2004). This scenario may not apply to SN 2008iy, however, because the ∼400 day rise time implies that the CSM density may have been increasing with radius, in which case the blast wave may have been continually decelerated during the rise.

Following the above assumptions, we can use equation (1) to determine the mass loss traced by the optical luminosity at a number of different epochs of interest. At each epoch, we determine the radius, $R = V_{SN} t_{SN} \approx 5000\,\mathrm{km\,s^{-1}}\ t_{SN}$, and the luminosity based on the light curve shown in Fig. 1. We do not adopt the bolometric correction determined in Section 3.1 for two reasons: (i) it is unclear whether this same correction is valid at early times and (ii) emission from an NIR echo should not be incorporated into equation (1), as that contribution to the total luminosity is not directly the result of CSM interaction. Thus, the estimates below of the luminosity do not reflect any emission from dust. At early times, day ∼153, $L \approx 6.8 \times 10^8\,\mathrm{L_\odot}$, which corresponds to $\dot{M} \approx 1.3 \times 10^{-2}\,\mathrm{M_\odot\,yr^{-1}}$ at $R \approx 6.6 \times 10^{15}$ cm, while at the time of peak $L \approx 1.2 \times 10^9\,\mathrm{L_\odot}$, $R \approx 1.7 \times 10^{16}$ cm and $\dot{M} \approx 2.3 \times 10^{-2}\,\mathrm{M_\odot\,yr^{-1}}$. On day 563, coincident with our X-ray observations of SN 2008iy the optical luminosity was $L \approx 7 \times 10^8\,\mathrm{L_\odot}$, which corresponds to $R \approx 2.4 \times 10^{16}$ cm and $\dot{M} \approx 1.3 \times 10^{-2}\,\mathrm{M_\odot\,yr^{-1}}$. On day 714, roughly coincident with our high-resolution Keck spectrum, $L \approx 4 \times 10^8\,\mathrm{L_\odot}$, $R \approx 3.0 \times 10^{16}$ cm and $\dot{M} \approx 0.8 \times 10^{-2}\,\mathrm{M_\odot\,yr^{-1}}$.

These results are quite remarkable; they suggest that at a time $t \approx V_{SN} t_{SN}/v_w \approx 5000\,\mathrm{km\,s^{-1}} \times 400\ \mathrm{d}/100\,\mathrm{km\,s^{-1}} \approx 55$ yr prior to the explosion of SN 2008iy the progenitor underwent a period of heightened mass loss. This enhanced mass-loss period was then followed by a period of decreasing mass loss leading up to the time of the SN explosion. While the quantitative results for the mass loss discussed above are sensitive to our adopted quantities, most specifically the progenitor wind speed and the speed of the SN blast wave, the fact remains that the continuum luminosity did increase over a period of ∼400 d after the SN explosion. Rearrangement of equation (1) shows that this luminosity increase is proportional to the wind-density parameter, $w = \dot{M}/v_w$. Thus, w must have *increased* over a distance $R \approx V_{SN} t_{SN} \approx 1.7 \times 10^{16}$ cm from the progenitor, regardless of the true wind speed over that distance. An increasing value of w means that during roughly the century prior to the SN there was a significant change in the wind properties of the progenitor.

Using our X-ray detection of SN 2008iy, we have an alternative method to probe the mass-loss history of the progenitor on day ∼563. Following Immler & Kuntz (2005), the X-ray luminosity may be written as

$$L_X = \frac{4}{(\pi m)^2}\Lambda(T)\left(\frac{\dot{M}}{v_w}\right)^2 (V_{SN} t)^{-1}, \quad (2)$$

where L_X is the X-ray luminosity, m is the mean mass per particle ($m = 2.1 \times 10^{-24}$ g for an H+He plasma), $\Lambda(T)$ is the cooling function of a plasma heated to temperature T, $\dot{M}$ is the mass-loss rate of the progenitor, v_w is the wind speed of the progenitor (∼100 km s^{-1}, see above), V_{SN} is the speed of the SN blast wave (∼5000 km s^{-1}, see above) and t is the time since explosion, ∼563 d. Assuming a temperature $T = 10^7$ K, appropriate for an optically thin thermal plasma (Immler & Kuntz 2005), the effective cooling function is $\Lambda(T) = 3 \times 10^{-23}\,\mathrm{erg\,cm^3\,s^{-1}}$. The X-ray luminosity on day 563 was $L_X \approx 2.4 \times 10^{41}\,\mathrm{erg\,s^{-1}}$. Substituting these values into equation (2), we find $\dot{M} \approx 0.7 \times 10^{-2}\,\mathrm{M_\odot\,yr^{-1}}$, which shows agreement with the value derived from the optical continuum, $\sim 1.3 \times 10^{-2}\,\mathrm{M_\odot\,yr^{-1}}$, given the uncertainty in a number of the assumptions we have adopted.

An additional estimate of the mass-loss rate of the progenitor comes from the narrow Hα emission seen in our Keck spectrum on day 711. Chugai & Danziger (2003) show that the Hα emission from the unshocked CSM is related to w:

$$L(\mathrm{H}\alpha) = \frac{1}{4\pi r_1}\alpha_{32} h\nu_{23} (x X w N_A)^2 \left(1 - \frac{r_1}{r_2}\right), \quad (3)$$

where r_1 is the inner radius corresponding to the position of the SN blast wave, r_2 is the outer radius related to the fast-moving forward shock, α_{32} is the effective recombination coefficient for Hα, $h\nu_{23}$ is the energy of an Hα photon, x is the degree of H ionization, X is the hydrogen mass fraction and N_A is Avogadro's number. We cannot constrain x, X or r_2, so we conservatively adopt $x = 1$, $X = 1$ and $r_2 \gg r_1$, all of which have the effect of minimizing w. Assuming Case B Hα recombination, $\alpha_{32} = 8.64 \times 10^{-14}\,\mathrm{cm^3\,s^{-1}}$, which is appropriate assuming that the narrow emission comes from photoionized gas. Substituting the narrow Hα luminosity [$L(\mathrm{H}\alpha) = 2.8 \times 10^{39}\,\mathrm{erg\,s^{-1}}$] and $r_1 = V_{SN} t_{SN} = 3.0 \times 10^{16}$ cm into equation (3), we find that $w \approx 10^{17}$ g cm^{-1}. With $v_w = 100\,\mathrm{km\,s^{-1}}$ on day 711, this corresponds to $\dot{M} \approx 1.6 \times 10^{-2}\,\mathrm{M_\odot\,yr^{-1}}$. At a similar epoch (see above), we find $\dot{M} \approx 0.8 \times 10^{-2}\,\mathrm{M_\odot\,yr^{-1}}$ based on the optical luminosity. Again, the agreement between these two methods to within a factor of ∼2 is reasonable given the uncertainties in our adopted parameters.

4.2 Late-time emission and the similarity to SN 1988Z

To explain the late-time (i.e. post peak) emission from SN 2008iy, we adopt a model that is virtually identical to that developed by Chugai & Danziger (1994) for SN 1988Z: the CSM contains optically thick clumps in addition to a rarefied wind between these clumps (see e.g. fig. 1 of Chugai & Danziger 1994). As the SN ejecta sweep through the CSM, they drive a fast-moving forward shock into the rarefied wind. This shocked material forms a cool dense shell between the forward and reverse shocks, and gives rise to the broad emission component seen in Hα (FWHM $\approx 5000\,\mathrm{km\,s^{-1}}$ for SN 2008iy). At the same time, a slower shock is being driven into the dense clumps, which leads to the intermediate-width emission (FWHM $\approx 1650\,\mathrm{km\,s^{-1}}$ in the case of SN 2008iy) seen in the spectra. The narrow P Cygni profile results from the pre-shock photoionized wind.

The observed similarities between SN 2008iy and SN 1988Z provide further evidence that comparable models are appropriate for the two SNe. In addition to having similar spectra at late times (see Fig. 3), SNe 1988Z and 2008iy have large X-ray luminosities (both SNe have $L_X \gtrsim 10^{41}\,\mathrm{erg\,s^{-1}}$; Fabian & Terlevich 1996, this work), and similar late-time decline rates [∼0.3–0.5 mag (100 d)$^{-1}$ in the optical; Turatto et al. 1993; this work], which in both cases are slower than the expected bolometric decline of radioactive ^{56}Co. Estimates for the mass-loss rate from the progenitor of SN 1988Z vary by roughly an order of magnitude. From X-ray observations, Schlegel & Petre (2006) find $\dot{M}_{1988Z} \approx 10^{-3}\,\mathrm{M_\odot\,yr^{-1}}$, while

Williams et al. (2002) estimate $\dot{M}_{1988Z} \approx 10^{-4}\,M_\odot\,yr^{-1}$ based on radio observations, and the models of the optical emission by Chugai & Danziger (1994) yield $\dot{M}_{1988Z} \approx 7 \times 10^{-4}\,M_\odot\,yr^{-1}$. While these estimates are one to two orders of magnitude less than those for SN 2008iy, we note that in each of the above estimates for $\dot{M}_{1988Z}$ a wind speed of $10\,km\,s^{-1}$ was adopted for the progenitor of SN 1988Z. If SN 1988Z had a progenitor wind speed closer to $\sim$100 km s^{-1}, a very reasonable possibility given the wind speed of SN 2008iy and other similarities between the two SNe, this would result in an increase in the estimated mass loss for the progenitor by a factor of $\sim$10, thereby bringing the estimates for the two SNe into accord.

Based on the late-time emission, SN 2008iy seems to belong to the group of SNe IIn that exhibit a slow evolution sustained by long-lived ($\gtrsim$1 decade) CSM interaction. In addition to SN 1988Z, other members of this group include SN 1986J (Rupen et al. 1987), SN 1995N (Fox et al. 2000; Fransson et al. 2002) and possibly also the VLSN 2003ma (Rest et al. 2009). Both SN 1986J and SN 1995N exhibit evidence for a clumpy progenitor wind, like SN 2008iy and SN 1988Z. Chugai (1993) modelled the X-ray emission from SN 1986J as the interaction between the SN ejecta and a clumpy wind (though note that Houck et al. 1998 prefer a model with a smooth CSM, but they conclude that they cannot rule out the clumpy model). The evidence for a clumpy wind from the progenitor of SN 1995N comes from both the optical spectra (Fransson et al. 2002) and the X-ray emission (Zampieri et al. 2005). Also, the optical decline of both SNe 1986J and 1995N is very slow: SN 1986J declined by $\lesssim$1 mag in the optical between 1994 and 2003 (Milisavljevic et al. 2008), while the *V*-band decline of SN 1995N was only 2.2 mag between 1998 and 2003 (Zampieri et al. 2005).

The duration of the interaction means that the large mass-loss rates from the respective progenitors must have been sustained for at least $\sim$100 yr prior to core collapse after the conservative assumption that $V_{SN} = 1000\,km\,s^{-1}$ and $v_w = 100\,km\,s^{-1}$. Typically, the blast wave continues to expand at $>1000\,km\,s^{-1}$ (SN 1988Z had a broad component that remained nearly constant at $\sim$2000 km s^{-1} from day $\sim$1500 to 3000; Aretxaga et al. 1999), which would make this time period $>$100 yr. These very long-lived SNe IIn are therefore connected in that their progenitors experienced lengthy periods with high mass-loss rates. This stands in stark contrast to the Type IIn SN 1994W, which had a light curve with an abrupt drop $\sim$100 d post explosion (Sollerman, Cumming & Lundqvist 1998). The mass loss from the progenitor of SN 1994W has been modelled to occur in a short ($\lesssim$1 yr), violent episode (Chugai et al. 2004), and the sudden drop in the light curve occurs because the SN ejecta have overtaken the dense CSM, thereby halting any interaction luminosity.

4.3 Origin of the 400-d rise time and implications for the progenitor

With a model to account for the late-time emission from SN 2008iy, we are still left with the puzzle of explaining the 400-d rise time.[6] This rise in the optical is significantly longer than that seen in any other known SN. As previously discussed, this scenario is possible if the progenitor underwent a phase of enhanced mass loss $\sim$55 yr prior to the SN explosion. The optical luminosity traces the wind-density parameter, w, meaning that during the decades prior to explosion either (i) the mass-loss rate declined or (ii) the wind speed increased, or (iii) both.

Episodic periods of enhanced mass loss, sometimes in the form of a shell ejection, have been observed for numerous luminous blue variables (LBVs; see Humphreys & Davidson 1994), though the underlying physics of these eruptions is not currently well understood (see Smith & Owocki 2006). If the progenitor of SN 2008iy had a giant eruption (similar to that of LBVs) $\lesssim$1 century prior to explosion, this could result in a density profile that peaks $\sim 1.7 \times 10^{16}$ cm from the progenitor. In the clumpy-wind scenario described in Section 4.2, this would mean that the ejecta are expanding into a wind where the number density of clumps is increasing with radius. Thus, as more and more clumps are overtaken by the ejecta, the continuum luminosity continues to rise, until after $\sim$400 d when the ejecta have reached $\sim 1.7 \times 10^{16}$ cm, the number density of clumps begins to decline and so does the optical luminosity. Alternatively, the long rise could result from the ejecta expanding into a non-spherical wind, such as a bipolar outflow, though this hypothesis would need to be examined with detailed hydrodynamical models.

The inferred mass-loss rate for SN 2008iy, $\dot{M} \approx 10^{-2}\,M_\odot\,yr^{-1}$, is similar to that for the first LBV, P Cygni, during its great eruption ($\dot{M}_{PCyg} \approx 10^{-2}\,M_\odot\,yr^{-1}$ during the 1600 AD eruption; Smith & Hartigan 2006). Furthermore, the terminal wind speed in the P Cygni nebula is 185 km s^{-1} (Lamers et al. 1996; Najarro, Hillier & Stahl 1997), which is similar to the observed BVZI for the narrow blue absorption seen in SN 2008iy, corresponding to $v_w \approx 160$–$450\,km\,s^{-1}$. We illustrate these comparisons to show that derived properties of the progenitor wind of SN 2008iy are similar to the giant eruption of a Galactic LBV; we are not insinuating that the great outburst from P Cygni is a direct analogue to the proposed LBV-like eruption from SN 2008iy. Such eruptions are not expected from RSGs.

Further evidence that the progenitor of SN 2008iy could not have had an RSG progenitor comes from the observed narrow P Cygni Hα profile. RSGs have typical wind speeds of $\sim$10 km s^{-1}, with extreme RSG winds reaching 40 km s^{-1} (see Smith et al. 2007). The observed 100 km s^{-1} wind speed from SN 2008iy is more characteristic of LBVs (e.g. P Cygni, see above) or the escape velocity from a blue supergiant. Similar $\sim$100 km s^{-1} P Cygni profiles have been seen in a number of SNe IIn, such as SNe 1997ab (Salamanca 2000), 1997eg (Salamanca et al. 2002), 1998S (Fassia et al. 2001) and 2007rt (Trundle et al. 2009), implying that the progenitors of each of these SNe may have been in a similar state shortly before core collapse.

The dense CSM and large luminosities associated with many SNe IIn have led a number of authors to suggest that at least some SNe IIn are associated with progenitors that experienced LBV-like mass loss shortly before core collapse (see e.g. Chu et al. 1999; Salamanca 2000; Chugai & Danziger 2003; Chugai et al. 2004). This possible connection was considerably strengthened following the direct identification of the progenitor of the normal Type IIn SN 2005gl on archival *Hubble Space Telescope* images (Gal-Yam et al. 2007; Gal-Yam & Leonard 2009). While the diagnostics above are not ubiquitous for all SNe IIn,[7] many of the signatures (high-density CSM, episodic mass loss with $\dot{M} \approx 10^{-2}\,M_\odot\,yr^{-1}$ and $\sim$100 km s^{-1} progenitor wind speed) are shared with SN 2008iy, suggesting that it too had an LBV-like progenitor.

[6] We have no spectra of the SN while it was still on the rise, thus we have no way of knowing if the SN underwent significant spectral evolution prior to day 560.

[7] Note that the low-resolution spectrographs typically employed to observe SNe lack sufficient resolution to resolve narrow (FWHM $\lesssim 150\,km\,s^{-1}$) absorption lines.

As mentioned above, an alternative way to generate a wind-density parameter that is increasing with distance from the progenitor is to increase the progenitor wind speed in the years leading up to the SN event. A relatively mild change in the wind speed by a factor of ∼3 could, in fact, explain the observed increase in luminosity. During the post-main-sequence evolution of very massive stars, a slightly more extreme transition is expected as stars exit the RSG or LBV phase, with wind speeds of ∼10–100 km s^{-1}, to become Wolf–Rayet stars, with typical wind speeds of $\gtrsim$1000 km s^{-1}. As this fast wind expands into the slower wind, it will sweep up a thin, dense shell at the interface of the two winds and thus create a wind-blown bubble (e.g. Dwarkadas 2005). A SN exploding in one of these bubbles will appear as a normal SN until the ejecta reach the edge of the bubble. As the ejecta overtake the thin shell, the appearance of the SN will dramatically change as CSM interaction begins to provide a significant contribution to the broad-band luminosity. This is the precise scenario proposed for the Type IIn SN 1996cr, for which Bauer et al. (2008) found an optical luminosity that is clearly decreasing between 1996 and 1999, but the radio emission sharply increases in late 1997 while X-ray emission abruptly turns on some time between 1998 March and 2000 January. The X-ray emission is especially interesting because after the abrupt initial rise it continues to rise for at least the next 7 yr, a feature which had not previously been observed for any X-ray SN. A similar scenario is proposed for SN 2001em, classified as a Type Ic, but which showed unexpectedly strong radio and X-ray emission >2 yr after explosion, as well as an FWHM ≈ 1800 km s^{-1} Hα emission line (Soderberg, Gal-Yam & Kulkarni 2004). Each of these late-time peculiarities can be understood if the progenitor of SN 2001em lost the remainder of its hydrogen envelope during a phase of large mass loss ∼(2– 10) × 10^{-3} M$_\odot$ yr^{-1}, about (1–2) × 10^3 yr prior to core collapse (Chugai & Chevalier 2006). After the hydrogen envelope has been lost, a fast wind from the progenitor sweeps the hydrogen into a shell. The interaction of the Type Ic ejecta with this swept-up shell gives rise to the unusual late-time emission.

Can the long optical rise be the result of SN 2008iy exploding inside a wind-blown bubble? There is a somewhat sharp rise in the optical (>2 mag brightening during the 68 d between the last DS non-detection and the first CRTS detection of the SN) followed by a slow and steady increase over the next ∼400 d, which may hint that the SN exploded in such a wind-driven cavity. However, we do not favour this model. In the wind-blown bubble scenario, after peak the thin shell has been overtaken by the ejecta, and the luminosity is powered by the interaction of the ejecta with the slower, older wind. To explain this, the wind on day 711 requires $\dot{M} \approx 10^{-2}$ M$_\odot$ yr^{-1} and $v_w \approx 100$ km s^{-1}, which requires LBV-like mass loss (see above). The wind-blown bubble scenario therefore seems to unnecessarily complicate the scenario discussed above, which is needed to explain the late-time observations, as it requires the transition from an LBV to a Wolf–Rayet star. Yet, the addition of this transition does not clearly model any observed properties that could not otherwise be explained.

Additionally, we see no evidence for a normal SN in the years leading up to the initial detection of SN 2008iy as would be expected in the wind-blown bubble scenario. While it would be impossible to completely rule out an SN prior to the first detection of SN 2008iy on 2007 September 13 (for instance, the field is virtually unobservable for ∼3 months each year while it is behind the Sun), DS images dating to 2004 show no evidence for such an event. These DS images have similar depths to those quoted in Section 2.1, which at the distance of the host galaxy corresponds to an absolute magnitude of $M_i \approx -15.4$ mag. This detection threshold is well below the mean peak magnitude for stripped envelope SNe: $M_R = -17.01$, -16.38 and -17.04 mag for SNe Ib, Ic and IIb, respectively [Li et al., in preparation(a)]. Stronger constraints on the presence of a stripped envelope SN prior to 2007 September 13 are based on the individual DS images. There are DS images of the field of SN 2008iy from 2004 April and July, 2005 May, June and July, 2006 May and June and 2007 April, May, June and July. Adopting the mean peak magnitudes and mean light curves for stripped envelope SNe from Li et al. [in preparation(a)], we find that on average (note that there is a great deal of dispersion in the peak absolute magnitude and duration of stripped envelope SNe) SNe Ib and IIb are observable for ∼70 d above the DS detection threshold, while SNe Ic are observable for only ∼45 d above the DS detection threshold. In addition to not being detected during any of the months listed above, we can also rule out SNe Ib and IIb in the ∼2 months prior to those listed above, while SNe Ic can be ruled out in the ∼1.5 months prior to those above. Therefore, in the ∼3.5 yr prior to SN 2008iy we can rule out SNe Ib or IIb in ∼21 out of 42 months, while SNe Ic can be ruled out for ∼18 out of 42 months.

Perhaps the most intriguing points about the progenitor of SN 2008iy are the implications for the progenitors of the very long lived SNe IIn discussed in Section 4.2, such as SN 1988Z. It is interesting that episodic, LBV-like eruptions, which we argue occurred shortly before SN 2008iy, may be applicable to SNe 1988Z, 1995N and 1986J, each of which has relatively poor constraints on the actual date of explosion.

SN 1988Z was first observed after peak (Stathakis & Sadler 1991), with an observational constraint on the rise time of <250 d (Turatto et al. 1993). It was argued by Turatto et al. (1993) that the rise time of SN 1988Z must have been short, in part because at the time no other known SN looked quite like SN 1988Z. SN 2008iy, which is a virtual clone of SN 1988Z at late times, does provide an example of an SN with a long rise time and a peak absolute magnitude that is brighter than the discovery magnitude of SN 1988Z. This negates the necessity of a short rise to peak for SN 1988Z. We submit that it is possible that SN 1988Z had a long rise time, though we note that with no observations during the 250 d prior to discovery there is no way to definitely prove this claim one way or another. A long rise to peak would, however, further strengthen the similarity of SN 2008iy and SN 1988Z.

Similarly, SNe 1986J and 1995N have poor constraints on the rise time. SN 1986J was discovered in the radio, with constraints on the explosion date ranging from 1982 to 1984; constraints on the optical rise are even worse, owing in part to the large extinction in the host galaxy, $A_V \approx 2$ mag (see Rupen et al. 1987). Typically, ∼10 months prior to discovery is adopted as the explosion date for SN 1995N (see Fox et al. 2000). However, this age of 10 months is based on the Hα profile of SN 1995N, which looked similar to the Hα profile of SN 1993N 10 months after SN 1993N had been discovered (Benetti, Bouchet & Schwarz 1995). We note that SNe IIn are a very heterogeneous subclass, and in our experience spectral ages of SNe IIn are not reliable, especially at times greater than a few months. Thus, poor optical constraints mean that SNe 1986J, 1988Z and 1995N all may have had long rise times, by the standards of typical SNe II whose rise times are $\lesssim$1 week [Li et al., in preparation(a)].

4.4 Similarities to very luminous SNe IIn

The long rise time and broad, symmetric evolution of SN 2008iy around peak optical emission is reminiscent of the Type IIn VLSNe 2006gy and 2008fz (Ofek et al. 2007; Smith et al. 2007; Drake

et al. 2009b). Applying the 'shell shock' model of Smith & McCray (2007), which was originally developed to explain the light curve of SN 2006gy, does not provide a physically plausible scenario for SN 2008iy because the relatively low $\dot{M}$ and large radius at peak imply that the CSM shell was not opaque. The 'shell shock' model argues that the extreme luminosity of these SNe is powered via a shock running into a dense, optically thick shell. Radiation from the shock is thermalized by the optically thick gas and must diffuse out of the shell.

Nevertheless, SN 2008iy does share a few similarities with the VLSNe IIn. Like SNe 2006gy and 2006tf, SN 2008iy shows evidence for a $\sim$100 km s^{-1} pre-shock CSM wind (see Smith et al. 2007, 2008a), and like SNe 2006gy, 2006tf and 2008fz, SN 2008iy experienced a period of enhanced mass loss during the decades prior to explosion. The difference between these systems is that the mass-loss rate from SN 2008iy, $\dot{M} \approx 0.01\,\mathrm{M}_{\odot}\,\mathrm{yr}^{-1}$, was less extreme than that from SNe 2006gy, 2006tf, 2008fz, where $\dot{M} \approx 1.0\,\mathrm{M}_{\odot}\,\mathrm{yr}^{-1}$ (e.g. Smith et al. 2010). Also, the time between the period of enhanced mass loss and the SN was longer for SN 2008iy, $\sim$55 yr, than for SNe 2006gy and 2006tf, $\lesssim$10 yr (Smith et al. 2010, 2008a). The result of these differences is that SN 2008iy did not reach as extreme as a peak luminosity and took considerably more time to reach peak optical output than the VLSNe IIn. Finally, if the late-time NIR excess is the result of an IR dust echo this would be similar to SN 2006gy (Smith et al. 2008b; Agnoletto et al. 2009; Miller et al. 2010). Smith et al. (2008b) and Miller et al. (2010) argue that a giant eruption $\gtrsim$1000 yr prior to SN 2006gy could potentially create the dust shell giving rise to the echoes, and a similar shell around SN 2008iy may explain the observed NIR excess.

The connection between VLSNe and very massive stars, such as η Car, was first made by Smith et al. (2007) because the large mass-loss rates needed to explain the extreme optical luminosity are reminiscent of η Car during the great eruption of 1843. It is interesting to note that were η Car to explode as an SN today, its appearance would be less like the VLSNe IIn discussed above and more similar to SN 2008iy. The reason for this is that with the eruption happening >150 yr ago, the ejected shell surrounding η Car has had sufficient time to expand ($R \approx$ few $\times\ 10^{17}$ cm) and become clumpy (Morse et al. 1998), with an optical depth that is now near unity (Davidson et al. 2001). Thus, η Car does not have the compact ($R \lesssim$ few $\times\ 10^{15}$ cm), very optically thick shell required to generate an extreme peak luminosity following an SN. Instead, as the SN ejecta sweep through the large shell,[8] they will successively overtake more and more mass within the clumpy CSM. This will likely give rise to a long rise time, similar to what was seen in SN 2008iy.

4.5 The host of SN 2008iy

At the adopted distance to SN 2008iy, our detection of the host galaxy in stacked SDSS images (see Section 2.3) means that the host has an absolute magnitude of $M_r \approx -13.7$ mag. This is significantly fainter than the Small Magellanic Cloud (with $M_V = -16.9$ mag). We do not detect narrow emission lines from the host in our SN spectra in order to make a direct measurement of the metallicity. The prospects for such a measurement in the near future are not good: if SN 2008iy continues to evolve like SN 1988Z, light from the SN may dominate over light from the host galaxy for years to come.

We can, however, estimate the metallicity based on the absolute magnitude of the host. Lee et al. (2006) use 27 dwarf irregular galaxies to determine the luminosity–metallicity relation for low-mass galaxies, and following from their equation (1) we find $12 + \log(\mathrm{O/H}) \approx 7.7$, assuming $M_B \approx M_r$. The uncertainty in this value is large, perhaps as great as $\pm$0.3 dex, based on both our assumption of $B - r = 0$ mag for the host and the substantial scatter in the luminosity–metallicity relationship for faint galaxies (Lee et al. 2006 find a scatter of 0.16 dex), yet this nevertheless shows that SN 2008iy occurred in a metal-poor galaxy.

It has recently been suggested that the unusual SNe discovered by the non-targeted transient surveys, such as CRTS, preferentially occur in subluminous, possibly metal-poor host galaxies (Drake et al. 2009b; Miller et al. 2009). SN 2008iy is yet another example of an unusual SN in a low-luminosity host. We caution, however, that a number of biases may be skewing initial impressions about the hosts of these unusual SNe. Preliminary calculations show that these VLSNe are rare (Miller et al. 2009; Quimby et al. 2009). Both the large peak luminosity and slow evolution of SN 2008iy mean that similar SNe would be easily detectable in the galaxies of targeted SN surveys. The lack of other examples of SNe with $\sim$400-d rise times suggests that SN 2008iy is also rare. The CRTS, however, does not employ image subtraction during their search for transients; instead, they use aperture photometry to find new sources, or sources with large increases in flux, and flag those as possible transients. Consequently, their survey is biased towards the discovery of intrinsically bright SNe in faint host galaxies. From the Lick Observatory Supernova Search (LOSS), we know that SNe IIn are rare, regardless of whether they are very luminous or have long rise times [Li et al., in preparation(b)]. Yet, even LOSS, which targets specific galaxies, may be biased in that it observes relatively few subluminous galaxies. New and upcoming surveys, such as the Palomar Transient Factory (Law et al. 2009; Rau et al. 2009), which employ image subtraction and survey large, non-targeted fields of view, will not suffer from the same biases discussed above, and hence will be in a better position to address whether these unusual SNe preferentially occur in subluminous host galaxies.

5 CONCLUSIONS

We have reported on observations of the Type IIn SN 2008iy, which took $\sim$400 d to reach peak optical output. There are few known SNe with optical rise times $\gtrsim$50 d, and SN 2008iy is the first with a rise time >1 yr. We argue that this long rise to peak is caused by the interaction of the SN ejecta with a dense CSM; radioactivity is unlikely to drive a 400-d rise. Furthermore, the late-time optical decay, $\sim$0.4 mag (100 d)$^{-1}$, is slower than that of ^{56}Co, which provides further evidence that radioactive heating is not a dominant energy source for SN 2008iy. Spectroscopically, SN 2008iy is very similar to SN 1988Z at late times. SN 1988Z is understood to have exploded in a dense, clumpy CSM (Chugai & Danziger 1994), which we argue was also the case for SN 2008iy. We detect SN 2008iy in X-rays with a total luminosity $L_{\mathrm{X}} = (3.7 \pm 1.2) \times 10^{41}$ erg s^{-1}, which is similar to that of the Type IIn SNe 1988Z and 1995N (Fox et al. 2000). Similar to other SNe IIn, SN 2008iy has a growing NIR excess at late times. SN 2008iy had a peak absolute magnitude of $M_r \approx -19.1$ mag and a total radiated energy of $\sim 2 \times 10^{50}$ erg in the optical (assuming no bolometric correction).

[8] The shell around η Car is much bigger than the one around SN 2008iy because the wind speeds are greater, $v_{w,\eta\mathrm{Car}} = 600$ km s^{-1} (Smith 2006), and the nebula is older, $\sim$165 yr relative to $\sim$55 yr.

The steady increase in optical luminosity over a ∼400-d period means that the wind-density parameter, w, increased over a distance of $\sim 1.7 \times 10^{16}$ cm from the SN. We propose two possible scenarios to explain this increase in w: (i) the progenitor experienced an episode of LBV-like, eruptive mass loss ∼55 yr prior to the SN or (ii) the wind speed of the progenitor was increasing during the years leading up to core collapse. We prefer the former scenario, as the later adds unnecessarily complicated pieces to the puzzle without providing a unique solution. Our favoured scenario provides yet another piece of evidence that some SNe IIn are connected to LBV-like progenitors (see Gal-Yam et al. 2007, and references therein). We find that the host of SN 2008iy is a subluminous dwarf galaxy, though we caution against premature conclusions that unusual SNe, specifically those that are very luminous or have very long rise times, preferentially occur in low-mass dwarf galaxies.

Finally, we close with some predictions for the late-time behaviour of SN 2008iy. There are examples of SNe IIn whose luminosity dramatically drops after the SN ejecta overtake the dense CSM (e.g. SN 1994W; Sollerman et al. 1998). However, the similarities to SN 1988Z suggest that SN 2008iy could continue interacting, and thus remain luminous, for several years. This would allow long-term monitoring in the radio, X-ray and optical, like SN 1988Z (Aretxaga et al. 1999; Williams et al. 2002; Schlegel & Petre 2006). We predict that SN 2008iy is a luminous radio source, like SN 1988Z (Van Dyk et al. 1993), though we note that at $z = 0.0411$ deep observations may be necessary for detection. The increasing K_s-band luminosity from day 560 to 710 is likely due to the presence of dust, and we predict that SN 2008iy will also be luminous in the mid-IR (∼3– 5 μm). The data are insufficient to distinguish between newly formed dust or dust that was present prior to the SN, but future medium- to high-resolution spectroscopy could distinguish between these two cases. If new dust is being formed, it should result in a systematic blueshift in the line profiles, as the dust creates an optically thick barrier to radiation from the receding SN ejecta.

ACKNOWLEDGMENTS

AAM would like to thank D. Poznanski for useful discussions that helped improve this paper and M. Modjaz for discussions concerning the metallicity of the host. We thank Neil Gehrels for approving the *Swift* ToO request for SN 2008iy, which was submitted by Dave Pooley, and the *Swift* team for scheduling and obtaining those observations. We acknowledge the use of public data from the *Swift* archive. Cullen Blake, Dan Starr and Emilo Falco assisted with the operation of PAIRITEL. We wish to thank the following Nickel observers: P. Thrasher, M. Kislak, J. Rex, J. Choi, I. Kleiser, J. Kong, M. Kandrashoff and A. Morton. We thank the referee, Nikolai Chugai, for suggestions that helped to improve this paper.

AAM is supported by the NSF Graduate Research Fellowship Programme and DOE grant DE-FC02-06ER41453. JSB's group is partially supported by National Aeronautics and Space Administration (NASA)/*Swift* grant NNX08AN84G. AVF's group is grateful for the financial assistance of NSF grant AST–0908886 and the TABASGO Foundation. PAIRITEL is operated by the Smithsonian Astrophysical Observatory (SAO) and was made possible by a grant from the Harvard University Milton Fund, the camera loan from the University of Virginia and the continued support of the SAO and UC Berkeley. The PAIRITEL project is partially supported by NASA/*Swift* Guest Investigator grant NNX08AN84G. This publication makes use of data products from the 2MASS, which is a joint project of the University of Massachusetts and the Infrared Processing and Analysis Center/California Institute of Technology, funded by the NASA and the NSF. Some of the data presented herein were obtained at the W. M. Keck Observatory, which is operated as a scientific partnership among the California Institute of Technology, the University of California and NASA; it was made possible by the generous financial support of the W. M. Keck Foundation. The authors wish to recognize and acknowledge the very significant cultural role and reverence that the summit of Mauna Kea has always had within the indigenous Hawaiian community; we are most fortunate to have the opportunity to conduct observations from this mountain.

NOTE ADDED IN PRESS

After this paper had been accepted, Chandra & Soderberg (2009) reported the radio detection of SN 2008iy in the 8.46 GHz band on 2009 December 26, which confirms our prediction that SN 2008iy would be a radio bright SN (see Section 5).

REFERENCES

Adelman-McCarthy J. K. et al., 2008, ApJS, 175, 297
Agnoletto I. et al., 2009, ApJ, 691, 1348
Aretxaga I., Benetti S., Terlevich R. J., Fabian A. C., Cappellaro E., Turatto M., della Valle M., 1999, MNRAS, 309, 343
Bauer F. E., Dwarkadas V. V., Brandt W. N., Immler S., Smartt S., Bartel N., Bietenholz M. F., 2008, ApJ, 688, 1210
Benetti S., Bouchet P., Schwarz H., 1995, IAU Circ, 6170
Bertin E., Arnouts S., 1996, A&AS, 117, 393
Bloom J. S., Starr D. L., Blake C. H., Skrutskie M. F., Falco E. E., 2006, in Gabriel C. et al., eds, Astronomical Data Analysis Software Systems XV. Astron. Soc. Pac., San Francisco, p. 751
Burrows D. N. et al., 2005, Space Sci. Rev., 120, 165
Butler N. R., Kocevski D., 2007, ApJ, 668, 400
Catelan M. et al., 2009, CBET, 1780
Chandra P., Soderberg A., 2009, ATel, 2362
Chu Y., Caulet A., Montes M. J., Panagia N., van Dyk S. D., Weiler K. W., 1999, ApJ, 512, L51
Chugai N. N., 1993, ApJ, 414, L101
Chugai N. N., Chevalier R. A., 2006, ApJ, 641, 1051
Chugai N. N., Danziger I. J., 1994, MNRAS, 268, 173
Chugai N. N., Danziger I. J., 2003, Astron. Lett., 29, 649
Chugai N. N., Blinnikov S. I., Fassia A., Lundqvist P., Meikle W. P. S., Sorokina E. I., 2002, MNRAS, 330, 473
Chugai N. N. et al., 2004, MNRAS, 352, 1213
Davidson K., Smith N., Gull T. R., Ishibashi K., Hillier D. J., 2001, AJ, 121, 1569
Drake A. J. et al., 2008, ATel, 1768
Drake A. J. et al., 2009a, ApJ, 696, 870
Drake A. J. et al., 2009b, ApJ, in press (arXiv:0908.1990)
Dwarkadas V. V., 2005, ApJ, 630, 892
Dwek E., 1983, ApJ, 274, 175
Fabian A. C., Terlevich R., 1996, MNRAS, 280, L5
Fassia A. et al., 2001, MNRAS, 325, 907
Filippenko A. V., 1982, PASP, 94, 715
Filippenko A. V., 1989, AJ, 97, 726
Filippenko A. V., 1997, ARA&A, 35, 309
Filippenko A. V., Halpern J. P., 1984, ApJ, 285, 458
Foley R. J., Smith N., Ganeshalingam M., Li W., Chornock R., Filippenko A. V., 2007, ApJ, 657, L105
Fox D. W. et al., 2000, MNRAS, 319, 1154
Fox O. et al., 2009, ApJ, 691, 650
Fransson C., Lundqvist P., Chevalier R. A., 1996, ApJ, 461, 993
Fransson C. et al., 2002, ApJ, 572, 350

Gal-Yam A., Leonard D. C., 2009, Nat, 458, 865
Gal-Yam A. et al., 2007, ApJ, 656, 372
Gerardy C. L. et al., 2002, ApJ, 575, 1007
Houck J. C., Bregman J. N., Chevalier R. A., Tomisaka K., 1998, ApJ, 493, 431
Humphreys R. M., Davidson K., 1994, PASP, 106, 1025
Immler S., Kuntz K. D., 2005, ApJ, 632, L99
Kalberla P. M. W., Burton W. B., Hartmann D., Arnal E. M., Bajaja E., Morras R., Pöppel W. G. L., 2005, A&A, 440, 775
Lamers H. J. G. L. M. et al., 1996, A&A, 315, L229
Law N. M. et al., 2009, PASP, 121, 1395
Lee H., Skillman E. D., Cannon J. M., Jackson D. C., Gehrz R. D., Polomski E. F., Woodward C. E., 2006, ApJ, 647, 970
Leonard D. C. et al., 2002, PASP, 114, 35
Li W., Van Dyk S. D., Filippenko A. V., Cuillandre J.-C., 2005, PASP, 117, 121
Li W., Jha S., Filippenko A. V., Bloom J. S., Pooley D., Foley R. J., Perley D. A., 2006, PASP, 118, 37
Mahabal A. A. et al., 2009, ATel, 2010
Martin D. C. et al., 2005, ApJ, 619, L1
Matheson T., Filippenko A. V., Ho L. C., Barth A. J., Leonard D. C., 2000, AJ, 120, 1499
Milisavljevic D., Fesen R. A., Leibundgut B., Kirshner R. P., 2008, ApJ, 684, 1170
Miller J. S., Stone R. P. S., 1993, Lick Observatory Technical Report No. 66. University of California, Santa Cruz
Miller A. A. et al., 2009, ApJ, 690, 1303
Miller A. A., Smith N., Li W., Bloom J. S., Chornock R., Filippenko A. V., Prochaska J. X., 2010, AJ, submitted (arXiv:0906.2201)
Morse J. A., Davidson K., Bally J., Ebbets D., Balick B., Frank A., 1998, AJ, 116, 2443
Najarro F., Hillier D. J., Stahl O., 1997, A&A, 326, 1117
Nugent P. E., 2009, BAAS, 41, 419
Ofek E. O. et al., 2007, ApJ, 659, L13
Oke J. B. et al., 1995, PASP, 107, 375
Pastorello A. et al., 2007, Nat, 447, 829
Patat F., Barbon R., Cappellaro E., Turatto M., 1993, A&AS, 98, 443
Poole T. S. et al., 2008, MNRAS, 383, 627
Pozzo M., Meikle W. P. S., Fassia A., Geballe T., Lundqvist P., Chugai N. N., Sollerman J., 2004, MNRAS, 352, 457
Prieto J. L. et al., 2007, AJ, submitted (arXiv:0706.4088)
Quimby R. M., Wheeler J. C., Höflich P., Akerlof C. W., Brown P. J., Rykoff E. S., 2007a, ApJ, 666, 1093
Quimby R. M., Aldering G., Wheeler J. C., Höflich P., Akerlof C. W., Rykoff E. S., 2007b, ApJ, 668, L99
Quimby R. M. et al., 2009, Nat, submitted (arXiv:0910:0059)
Rau A. et al., 2009, PASP, 121, 1334
Rest A. et al., 2009, ApJ, submitted (arXiv:0911.2002)
Roming P. W. A. et al., 2005, Space Sci. Rev., 120, 95
Rupen M. P., van Gorkom J. H., Knapp G. R., Gunn J. E., Schneider D. P., 1987, AJ, 94, 61
Salamanca I., 2000, Memorie della Societa Astronomica Italiana, 71, 317
Salamanca I., Terlevich R. J., Tenorio-Tagle G., 2002, MNRAS, 330, 844
Schlegel E. M., 1996, AJ, 111, 1660
Schlegel E. M., Petre R., 2006, ApJ, 646, 378
Schlegel D. J., Finkbeiner D. P., Davis M., 1998, ApJ, 500, 525
Skrutskie M. F. et al., 2006, AJ, 131, 1163
Smith N., 2006, ApJ, 644, 1151
Smith N., Hartigan P., 2006, ApJ, 638, 1045
Smith N., McCray R., 2007, ApJ, 671, L17
Smith N., Owocki S. P., 2006, ApJ, 645, L45
Smith N. et al., 2007, ApJ, 666, 1116
Smith N., Chornock R., Li W., Ganeshalingam M., Silverman J. M., Foley R. J., Filippenko A. V., Barth A. J., 2008a, ApJ, 686, 467
Smith N. et al., 2008b, ApJ, 686, 485
Smith N. et al., 2009, ApJ, 695, 1334
Smith N., Chornock R., Silverman J. M., Filippenko A. V., Foley R. J., 2010, ApJ, 709, 856
Soderberg A. M., Gal-Yam A., Kulkarni S. R., 2004, GCN, 2586
Sollerman J., Cumming R. J., Lundqvist P., 1998, ApJ, 493, 933
Stathakis R. A., Sadler E. M., 1991, MNRAS, 250, 786
Stetson P. B., 1987, PASP, 99, 191
Trundle C. et al., 2009, A&A, 504, 945
Turatto M., Cappellaro E., Benetti S., Danziger I. J., 1993, MNRAS, 265, 471
Van Dyk S. D., Weiler K. W., Sramek R. A., Panagia N., 1993, ApJ, 419, L69
Voges W. et al., 1999, A&A, 349, 389
Williams C. L., Panagia N., Van Dyk S. D., Lacey C. K., Weiler K. W., Sramek R. A., 2002, ApJ, 581, 396
Zampieri L., Mucciarelli P., Pastorello A., Turatto M., Cappellaro E., Benetti S., 2005, MNRAS, 364, 1419

This paper has been typeset from a TEX/LATEX file prepared by the author.